Journal of Power and Energy Systems

Vol.6, No.2, 2012

Numerical Simulation of Two-Phase Critical Flow with the Phase Change in the Nozzle Tube*

Masahiro ISHIGAKI**, Tadashi WATANABE**,*** and Hideo NAKAMURA**

** Japan Atomic Energy Agency

2–4 Shirakata-shirane, Tokai-mura, Naka-gun, Ibaraki 319–1195, Japan

E-mail: ishigaki.masahiro@jaea.go.jp

*** (present address) Research Institute of Nuclear Engineering, University of Fukui

1-2-4 Kanawa-cho, Tsuruga-shi, Fukui 914-0055, Japan

Abstract

Two-phase critical flow in the nozzle tube is analyzed numerically by the best estimate code TRACE and the CFD code FLUENT, and the performance of the mass flow rate estimation by the numerical codes is discussed. For the best estimate analysis by the TRACE code, the critical flow option is turned on. The mixture model is used with the cavitation model and the evaporation-condensation model for the numerical simulation by the FLUENT code. Two test cases of the two-phase critical flow are analyzed. One case is the critical flashing flow in a convergent-divergent nozzle (Super Moby Dick experiment), and the other case is the break nozzle flow for a steam generator tube rupture experiment of pressurized water reactors at Large Scale Test Facility of Japan Atomic Energy Agency. The calculation results of the mass flow rates by the numerical simulations show good agreements with the experimental results.

Key words : Two Phase Flow, Critical Flow, Phase Change, Numerical Simulation, Best Estimate Code TRACE, CFD Code FLUENT

1. Introduction

The two-phase flows are observed at a loss of coolant accident (LOCA) of light water reactors, and it is important to estimate the mass flow rate of the two-phase flow accurately for the safety analysis of LOCA. For example in the steam generator tube rupture (SGTR) accident of pressurized water reactors (PWRs), the two-phase critical flows are observed and the phase change of water occurs in the broken steam generator tube. The accurate assessment of the two-phase critical flow in the broken tube is necessary for analyzing SGTR transients. Some researches are reported about the numerical calculation of the two-phase critical flow by the best estimate (BE) code RELAP5 (e.g. Refs.(1)–(3)). Chung improved the critical flow model for the two-phase flow and calculated the small break LOCA simulation. Städtke et al.[4] developed the model of the two-phase flow simulation, and analyzed the two-phase critical flow numerically. They obtained the qualitatively valid results. However, the analysis of the critical flow by computational fluid dynamics (CFD) code is not reported so much.

In this research, the numerical analyses of the two-phase critical flow by the BE code "TRACE" and the CFD code "FLUENT" are compared with the experimental results, and we discuss the performance of the numerical codes. Two test cases of the two-phase critical flows are simulated numerically. First, we test the critical flashing flow in the convergent-divergent nozzle (Super Moby Dick experiment). This simulation is the benchmark test of the critical flow with the phase change, and the experimental result and the numerical result of the flow have been reported in the literature[5]. Secondly, we calculate the flow in the break nozzle for SGTR experiment at Large Scale Test Facility (LSTF) of Japan Atomic Energy Agency[2]. The mass flow rates, pressures and void fractions by the numerical simulations are compared with the experimental results.

*Received 31 Jan., 2012 (No. 12-0067)
[DOI: 10.1299/jpes.6.264]

2. Critical Flashing Flow in a Convergent-divergent Nozzle (Super Moby Dick Experiment)

2.1. Problem Description

The critical flashing flow is observed in a convergent-divergent nozzle (Super Moby Dick experiment), when the pressure difference between the inlet and the outlet is more than the critical value and the temperature of water is higher than the saturation temperature. The steady choked flow occurs and water flashes at the divergent area of the nozzle.

We compare the mass flow rate, the pressure and the void fraction in the convergent-divergent nozzle by our numerical simulations with the experimental results and the numerical results by the WAHA code shown in the paper by Tiselj et al.[5]. Figure 1 shows the area of the nozzle cross section used for the numerical simulation. The area at the inlet (the axial position x=0.0 m) is 3.5×10^{-3} m^2, that at the outlet (x=0.9 m) is 4.3×10^{-3} m^2, and that of the straight part is 3.1×10^{-4} m^2. The pressures and temperatures at the boundaries are set as the constant values shown in Table 1. The pressure and temperature are given at the inlet boundary, and the pressure is given at the outlet boundary. The transient flow field is calculated until the steady flow state is observed.

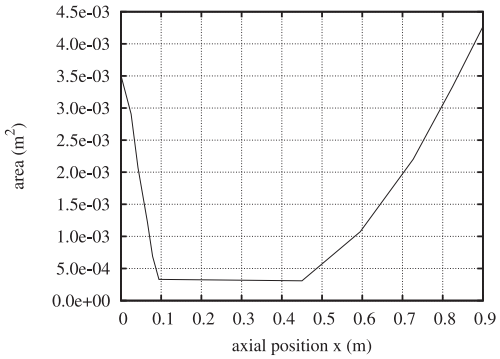

Fig. 1 The area of the nozzle cross section

Table 1 The boundary conditions for the simulation of the Super Moby Dick experiment

	pressure	temperature
inlet	8.0 MPa	549.6 K
outlet	4.7 MPa	-

2.2. Numerical Calculation by TRACE

The two-phase critical flow is analyzed by TRACE ver.5.0 patch 1[6]. The nozzle is divided to 30 nodes. The cell length is between 1.28 cm – 2.52 cm in the convergent part, 7 cm in the straight part. In the divergent part, the cell length is 1.176 cm (0.45 m$\leq x <$0.65 m) and 8.33 cm (0.65 m$\leq x \leq$ 0.9 m). The flow in the nozzle divided to 20 nodes is also calculated, and the difference of the results between the case with 20 nodes and 30 nodes is not observed. In this analysis, the two-phase critical flow option is used. The two-phase critical flow option included in the TRACE code is based on the Ransom and Trapp model[3]. In this model, the acoustic signals cannot propagate upstream at the position where flow area expands under the condition of the choking, and the critical flow is calculated by a characteristic analysis and the evaluation of the eigenvalues of the quasi-linear basic equations (mass, momentum, and energy conservation equations). The two-phase critical flow option is turned on at the position where the flow area increases along the flow direction, namely the last node of the straight part (the junction of the straight part and the divergent part, x=0.45 m). The calculation results in the case that the critical flow option is turned on at the last node of the straight part are almost

same as the results in the case that the critical flow option is turned on at all nodes of the divergent part.

2.3. Numerical Calculation by FLUENT

It is assumed that the flow in the nozzle is axisymmetric, and the flow is simulated in the 2D space. For the CFD analysis, FLUENT ver.12.0.16[7] is used. The mixture model is used to calculate the two-phase flow. The basic equations are the continuity equation, momentum equation, energy equation, volume fraction equation for the secondary phase, and algebraic expression for slip velocity. The density of water vapor is calculated as that of the ideal gas. The density of liquid water is calculated by Tait's equation[8] in Eq.(1):

$$\frac{p+B}{p_{ref}+B}=\left(\frac{\rho}{\rho_{ref}}\right)^{N} \tag{1}$$

where $B = 3.3 \times 10^8$ Pa and $N = 7.15$. In this research, we use two different values of the reference pressure p_{ref} and density ρ_{ref}. One set of p_{ref} and ρ_{ref} is the pressure and density at 1.013×10^5 Pa and 273.15 K (case 1). In this case, the reference values are $p_{ref} = 1.013 \times 10^5$ Pa and $\rho_{ref} = 999.8$ kg/m^3, respectively. The other case (case 2) used the values at the saturated state in the position. Namely, the density is calculated by Eq.(2)[8]:

$$\frac{p+B}{p_{sat}(T)+B}=\left(\frac{\rho}{\rho_{sat}(T)}\right)^{N} \tag{2}$$

where T is the local temperature, p_{sat} is the saturated pressure and ρ_{sat} is the saturated density of liquid water.

The phase change of water is simulated by the cavitation model in the FLUENT code (Schnerr and Sauer model) and the evaporation-condensation model implemented by the User Defined Function[9]. In the cavitation model, the mass transfer rate from the liquid to the vapor is evaluated by the bubble radius and the pressure. On the other hand, the mass transfer rate is evaluated by the difference between the temperature and the saturation temperature in the evaporation-condensation model. The Standard k-epsilon model and Standard Wall Functions are used for the effect of the turbulent flow[10]. We use these turbulent models because we choose the two-equations model as the standard turbulent models. In addition, these models are the simplest combination of the two-equations turbulent model so as to reduce the complicacy about the setting of the model parameters, while there is still large uncertainty about the choice of turbulent models for two-phase flow especially. The PISO scheme is used as the flow solution method. The spatial gradient terms are discretized by the least squares cell based method. The pressure interpolation scheme is the second order scheme. The convection terms of momentum and energy equations are discretized by the QUICK method for the higher accuracy calculation, and the convection terms of the other equations are discretized by the first order upwind scheme. All diffusion terms are discretized by the second order central differencing. These schemes are applied as standard combinations of the numerical calculation methods.

The computational mesh is generated by the mesh generator "GAMBIT" and the computational domain is divided into 8154 (453×18) rectangular elements. The size of the control volume is between 1.0×10^{-6} m^2–4.1×10^{-6} m^2.

For the two-phase flow calculation, the following procedures are done. First, the single-phase (liquid water) flow is calculated with turning off the mixture model. Second, the mixture model, the cavitation model and the evaporation-condensation model are turned on and the two-phase flow is simulated.

2.4. Numerical Results and Discussion

The mass flow rates by the experiment, the WAHA code[5], the TRACE code and the FLUENT code are shown in Table 2. The mass flow rate by the WAHA code and the FLUENT code in the case 1 show good agreements with that by the experiment. On the other hand, the

mass flow rate by the FLUENT code in the case 2 is about 21% smaller than the experimental result. The density in the case 2 is averagely smaller than that in the case 1, because the saturation density of liquid on the condition of this test (=the reference density in the case 2) is smaller than the density of the liquid at 0.1 MPa and 273.15 K (=the reference density in the case 1). Considering the liquid density has a axial distribution, the tendency that the volume flow rate in the nozzle is under estimated by the FLUENT code is shown. The mass flow rate by the TRACE code is about 13% smaller than that of experiment. This result is discussed later.

Table 2 The mass flow rates by the experiment, WAHA code, TRACE code, and FLUENT code

	mass flow rate (kg/s)
Experiment	16.99
WAHA	17.38
TRACE	14.72
FLUENT (case 1)	16.40
FLUENT (case 2)	13.46

Figure 2 shows the pressure distributions along the nozzle axis. The results by the experiment, the WAHA code, the TRACE code and the FLUENT code are plotted in Fig.2. The calculation result by the TRACE code is also plotted when the critical flow option is turned off. The numerical results except the result by the TRACE code without the critical flow option agree with the experimental result qualitatively. The result by the TRACE code shows the pressure has the minimum value at the end of the straight pipe where the critical flow option is active. In the simulations by the FLUENT code, the shock wave is observed at the middle of the divergent part of the nozzle. According to comparison of the pressure distributions by the FLUENT code in the both cases, the pressure have almost the same distributions and the positions of the shock wave are slightly different. The pressure oscillations behind the shock wave are observed in the pressure distributions by the FLUENT code. It is not clear that this pressure oscillation is observed at the experiment because of the shortage of the data point, and the pressure oscillation might be the numerical oscillation caused by the numerical scheme.

The void fraction distributions are shown in Fig.3. The vapor is generated in the divergent part of the nozzle. The void fractions in the divergent part by the FLUENT code and the TRACE code are over estimated. However, the void fraction by the FLUENT code can simulate the reduction tendency near the outlet. Figure 4 shows the void fraction distribution in the nozzle by the FLUENT code in the case 1. The vapor is generated almost homogeneously across the cross section of the nozzle.

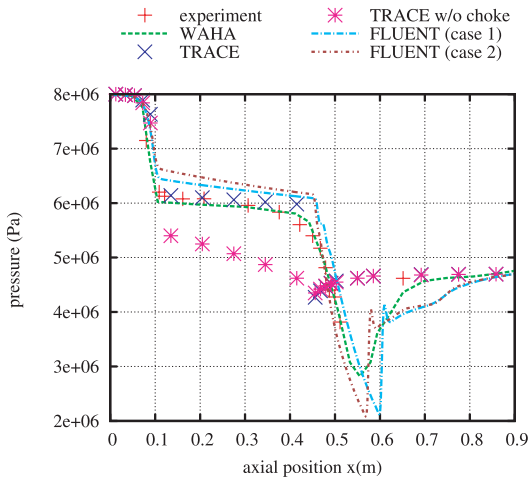

Fig. 2 The pressure distribution along the tube axis

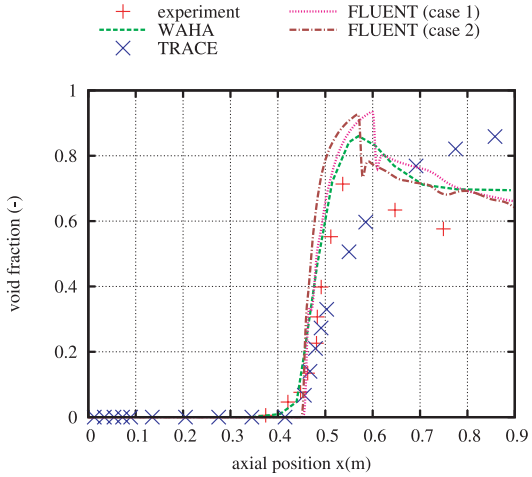

Fig. 3 The void fraction distribution along the tube axis

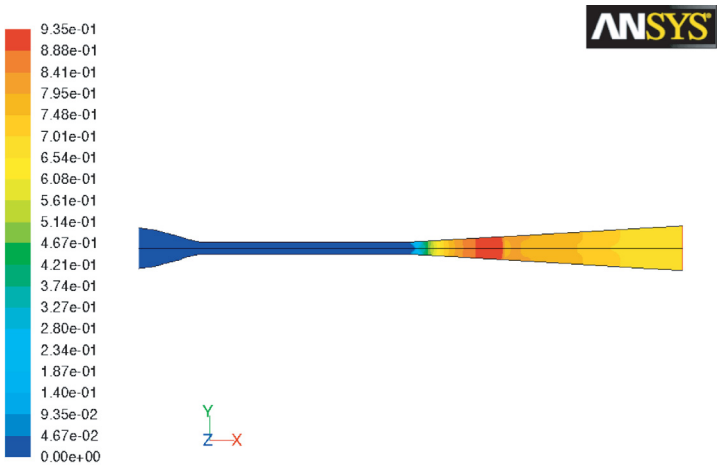

Fig. 4 The void fraction distribution in the nozzle by the FLUENT code (case 1)

Here, we consider the calculated results by the TRACE code. Firstly, we consider the difference between "WAHA code" and "TRACE code". The WAHA code is the computer code for simulations of the two-phase flow water hammer phenomena developed by Workpackage 2 of the WAHALoads project. The pressure distribution by the WAHA code is very similar to the pressure distribution by the FLUENT code with the shock wave. On the other hand, the pressure distribution by the TRACE code differs from those by the WAHA code and the FLUENT code, and the shock wave is not captured. In addition to that, the vapor generation models for the WAHA code and the TRACE code are different. The vapor generation term in the WAHA code is calculated by the homogeneous relaxation model. The generation term Γ is expressed by Eq. (3).

$$\Gamma = -\rho_m \frac{X - X_{sat}}{\theta} \tag{3}$$

where X is the vapor quality, X_{sat} is the quality at saturation, and ρ_m is the mixture density. θ is the relaxation time. The value of the generation term in the WAHA code is determined by the pressure and the saturation enthalpies. On the other hand, the vapor generation term in the TRACE code is evaluated from the heat conduction limited model by Eq. (4)[6].

$$\Gamma = -\frac{q_{iv} + q_{il}}{h_v - h_l} \tag{4}$$

where q_{iv} and q_{il} are the interfacial heat transfers per unit volume on the vapor and liquid sides, and h_v and h_l are the appropriate enthalpies of the vapor and liquid. The difference of the void fraction distributions might be observed because of the different vapor generation models between the WAHA code and the TRACE code. Since the numerical calculations by the WAHA code and the TRACE code are different in the pressure distribution, capturing the shock wave and the vapor generation, the difference of the mass flow rate could be observed between the result by TRACE code and that by the WAHA code.

In addition, the two-phase flow is calculated using two-fluid model in the TRACE code, and the flows of the gas phase and liquid phase are calculated in the each phase. It could be considered that capturing the position of the shock wave is difficult under the condition that the acoustic velocity is quite different between the gas phase and liquid phase. This may be one of the reason why the TRACE code cannot capture the shock wave.

The numerical results by the FLUENT code (mass flow rate, pressure, and void fraction) show relatively good agreements with those by the experiment and the WAHA code. On the other hand, the numerical results by the TRACE code are slightly different from those by the experiment. The TRACE code might not be able to calculate the shock wave in the divergent nozzle correctly.

3. Break Nozzle Flow for a SGTR Experiment at LSTF

3.1. Problem Description

In the previous section, we obtain the numerical results of the two-phase critical flashing flow, and it is shown the mass flow rate of the two-phase critical flow can be almost properly estimated by the FLUENT code. Then, we simulate the break flow experiment of PWR using the numerical codes. Especially, we focus on the break nozzle flow for a SGTR experiment at LSTF of Japan Atomic Energy Agency. This experiment (SB-SG-11) was done as one of the experiment of the ROSA-V project and was the model experiment of SGTR[(2)]. In this experiment, the pressure difference between the primary side of the steam generator (SG) and the secondary side of SG is kept so high that the two-phase critical flow is observed for a long time.

Figure 5 shows the schematic of the break nozzle for the SGTR experiment at LSTF. The SGTR accident is simulated by connecting the primary side of the SG and the secondary side with the break nozzle. The length of the break nozzle is 1800 mm and the inner diameter is 6.2 mm. Both sides of the break nozzle are wider than the break nozzle. For numerical simulation, the two-phase flows in this break nozzle are calculated. The measured values at the inlet and the outlet of the break nozzle are used as the boundary conditions for the numerical simulations. The measured pressures at the inlet and the outlet, and the temperature at the inlet are applied to the boundary conditions.

3.2. Numerical Calculation by TRACE

For the numerical calculation by the TRACE code, the break nozzle is discretized to 12 equally-spaced nodes in Fig.6. In this analysis, the two-phase critical flow option of the TRACE code is turned on at the last node of the break nozzle. In order to estimate the influence of the critical flow option, the flow when the critical flow option is turned off is also calculated.

3.3. Numerical Calculation by FLUENT

The numerical procedure by FLUENT is the same way as the calculation of the Super Moby Dick experiment. The 2D computational domain is divided into 9292 (2323 × 4) rectangular elements and all size of the control volume is 0.775 mm × 0.775 mm. The numerical results hardly change when the mesh with different control volume size is used, and the dependency of the flow models on the computational mesh is not observed in this case.

In this simulation, the steady state is simulated for the condition at 200 sec from the beginning of the SB-SG-11 experiment without calculating the transient flow. Because it is

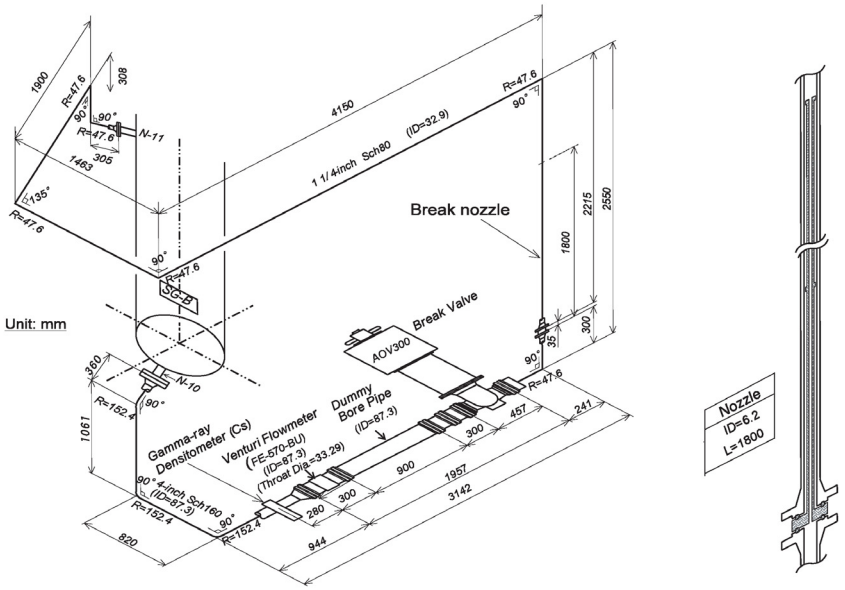

Fig. 5 Schematic of a break nozzle of the SGTR experiment

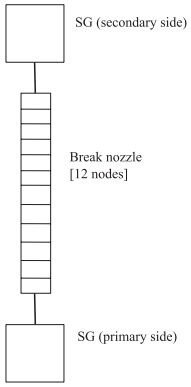

Fig. 6 The noding of the break nozzle

difficult to simulate the transient of the two-phase flow such as the break flow of LOCA by the FLUENT code and it takes for a very long time to calculate the transient flow, and the flow state can be assumed as the quasi-steady sate. The experimental values of the pressure and temperature at 200 sec from the beginning of the SB-SG-11 experiment are shown in Table 3. These pressure and temperature are used as the boundary conditions for the numerical simulation.

Table 3 The experimental values at 200 sec from the beginning of the SB-SG-11 experiment

	pressure	temperature
inlet	11.4 MPa	563 K
outlet	1.25 MPa	-

3.4. Numerical Results and Discussion

Here, the numerical results by the TRACE code are compared with the experimental results and the numerical results by the RELAP5 code in the literature[2]. The time histories of the mass flow rate in the break nozzle by the experiment and the TRACE code are shown in Fig.7. The numerical results by the TRACE code are the values when the critical flow option is turned on with the various numbers of the nodes (6 nodes, 12 nodes, 24 nodes) and

when the critical flow option is turned off with 12 nodes. The calculation results when the critical flow option is turned on with 12 nodes and 24 nodes have good agreements with the experimental result. If the number of the nodes for the numerical simulation is insufficient, the mass flow rate is probably over estimated. Since the pressure gradient might be over estimated using the insufficient nodes. The mass flow rate when the critical flow option is turned off is larger than those when the critical flow option is turned on. It is needed to turn on the critical flow option for the accurate estimation of the mass flow rate of the critical flow. Comparing with the calculation of Super Moby Dick experiment, the mass flow rates by the TRACE code show the quite better agreement with the experiment result. In the SGTR experiment, the shock wave is not observed in the nozzle, and the geometry of the nozzle is simple in contrast to the Super Moby Dick experiment nozzle. Therefore, it can be thought that the numerical results of the break nozzle flow for the SGTR experiment show the good agreement with the experimental results.

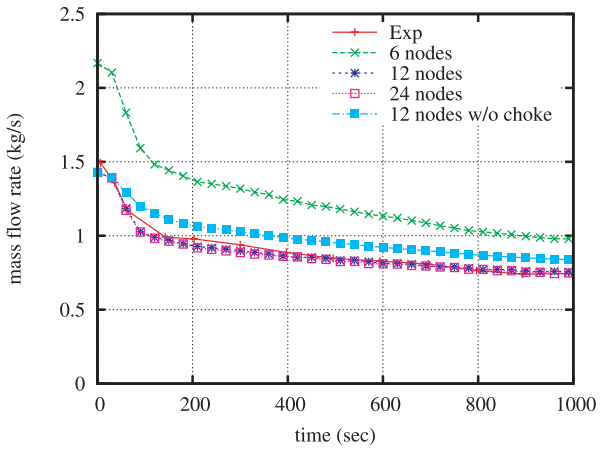

Fig. 7 The time history of the mass flow rate in the break nozzle

In Fig.8, the time histories of the pressure are shown. The pressures at the last node (outlet side) of the break nozzle by the TRACE code and the RELAP5 code[2] when the critical flow option is turned on or off, and the experimental pressures at the primary side and the secondary side of the steam generator (the boundary conditions of the pressure) are shown. The RELAP5 code is widely used for the safety analysis of the thermal hydraulic phenomenon, and the development and improvement of the code have been continued for a long time. For the analysis by the RELAP5 code, the RELAP5/MOD2 code was used and the nozzle was discretized to 12 equally-spaced nodes. The time histories of the pressure by the TRACE code almost agree with those by the RALAP5 code. Figure 9 shows the time histories of the void fraction by the TRACE code and the RELAP5 code. The void fractions at the 10th node, 11th node and 12th node (the last outlet side node) are shown. The void fractions by the TRACE code are under estimated than those by the RELAP5 code. The initiations of the phase change by the TRACE code are faster than those by the RELAP5 code at the 10th node and the 11th node. These differences might be caused by the difference of the correlation equations and/or flow models and so on, however, the detail of the cause is unclear. So, the further analyses by the TRACE code and the RELAP5 code are needed.

The mass flow rates by the FLUENT code and the experiment are shown in Table 4. The result of the case 1 is about 20 % larger and that of the case 2 is about 2 % larger than the experimental result. The improvement of the mass flow rate in the case 2 means that the volume flow rate is relatively over estimated by the FLUENT code and the mass flow rate is improved by the smaller liquid density in the case 2 in contrast to the simulation of the Super Moby Dick experiment.

Although the calculated result of the mass flow rate is improved by the adjustment of

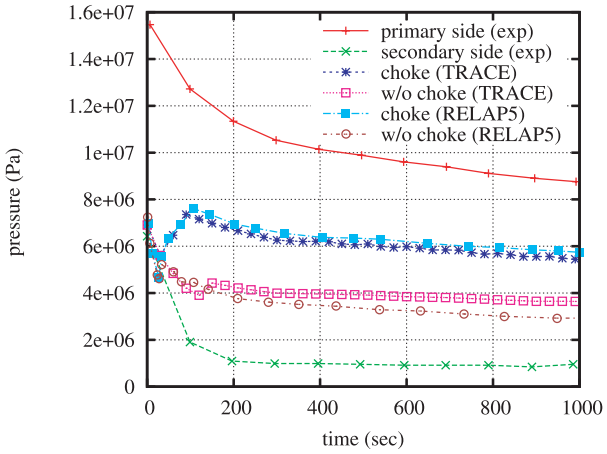

Fig. 8 The time history of the pressure in the break nozzle

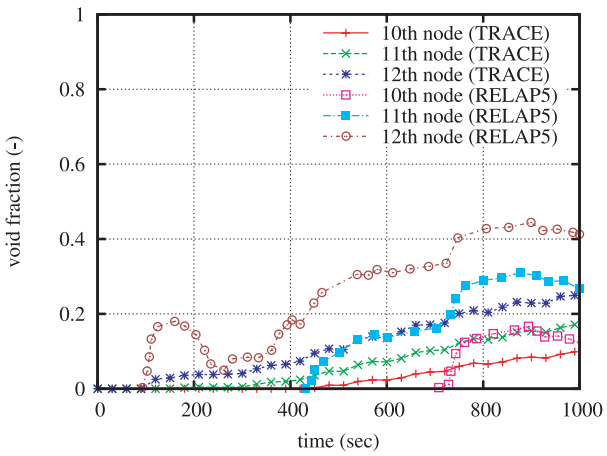

Fig. 9 The time history of the void fraction in the break nozzle

the liquid water density, the mass flow rates of the SGTR experiment are over estimated. The pressure difference between the inlet and the outlet of the nozzle in the simulation of the SGTR experiment is about 10 MPa and it is larger than that in the simulation of the Super Moby Dick experiment (about 3 MPa), so the influence of the compressibility for the analysis of the SGTR experiment is more crucial than that of the Super Moby Dick experiment. In the numerical calculation by the FLUENT code, the compressibility of vapor phase is simulated as that of the ideal gas. However, the compressibility of liquid phase is simulated approximately in the FLUENT code. Therefore, the mass flow rates by the FLUENT code might be over estimated than that by the experiment.

Table 4 The mass flow rates by the experiment and the FLUENT code

	mass flow rate (kg/s)
Experiment	0.965
FLUENT (case 1)	1.156
FLUENT (case 2)	0.981

In Fig.10, the pressure distribution along the nozzle axis by the FLUENT code in the case 2 is shown. A large pressure gradient is observed near the outlet of the nozzle. It is considered this large pressure gradient is caused by the effect of the critical flow at the outlet and the vapor generation by the phase change model. The influence of the position of the outlet boundary condition could be also considered as the cause. However, the information of the outside the outlet does not propagate into the nozzle under the condition of choking,

and the influence of the position of the outlet boundary could be considered small. It can be also considered that the outlet of the nozzle in the break flow is the position where the shock wave may occur if the outside tube of the outlet exists because the tube radius increases at the downstream area from the outlet of the nozzle. So, this effect might be cause of the large pressure gradient near the outlet. Figure 11 shows the void fraction distribution around the outlet of the break nozzle by the FLUENT code in the case 2. The phase change is only observed at the vicinity of the outlet, and it is caused by the cavitation of water. The vapor is generated almost homogeneously across the cross section of the nozzle. The phase change by the cavitation model occurs in the area where the pressure is lower than the saturation pressure. The pressure near the outlet substantially decreases in Fig.10. So, the high void fraction is observed near the outlet of the nozzle. The void generation has the interaction with the pressure distribution.

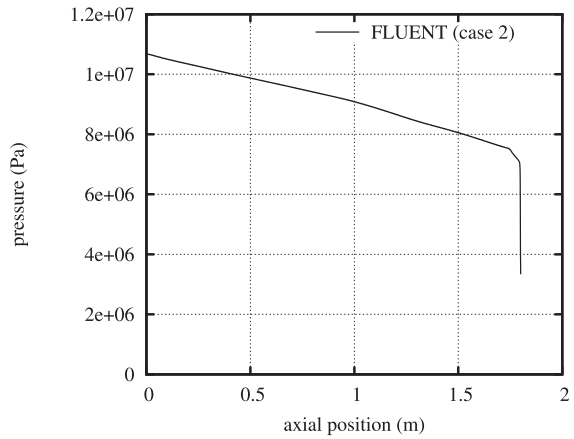

Fig. 10 The pressure distribution along the nozzle axis by the FLUENT code (case 2)

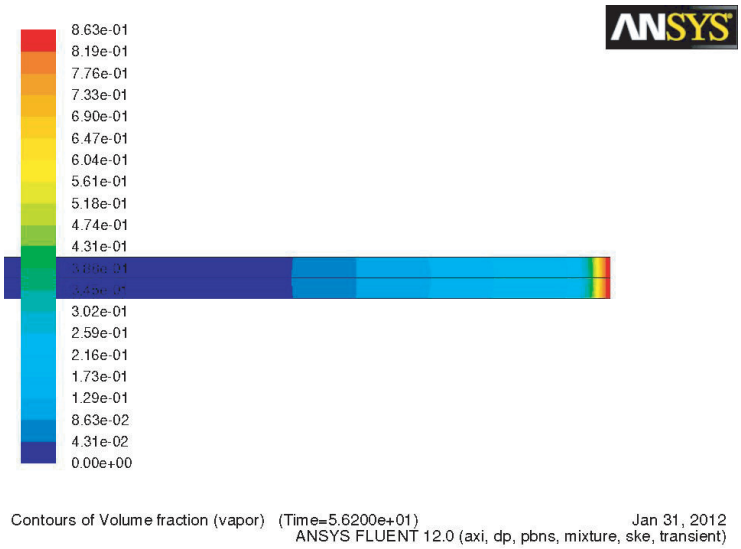

Fig. 11 The void fraction distribution near the outlet of the break nozzle by the FLUENT code (case 2)

4. Conclusions

The two-phase critical flows are analyzed by the TRACE code and the FLUENT code. For the numerical simulation of the steady critical flow with the shock wave, the mass flow

rate by the FLUENT code in the case using the constant density of liquid water as the reference density (case 1) shows good agreement with those by the experiment and the numerical code for the shock wave calculation (the WAHA code). However, the mass flow rates by the TRACE code and the FLUENT code in the case using the saturated density of liquid (case 2) are smaller than that by the experiment. It could be caused by the problem of capturing the shock wave and the vapor generation for the results by the TRACE code. On the other hand, for the numerical simulation of the transient critical flow, the mass flow rate by the TRACE code shows good agreement with those by the experiment and the RELAP5 code. The mass flow rate by the FLUENT code in the case 1 is larger than that by the experiment. However, the mass flow rate by the FLUENT code in the case 2 shows agreement with the experimental result.

The FLUENT code has the possibility that it is applicable to the detail simulation of the two-phase critical flows, and it would be available for the safety analysis. In order to estimate the physical properties of the two-phase critical flow more accurately, more detail analyses and simulations are needed.

References

(1) Chung, M.S., Simulation of SBLOCA Based on an Improved Choked Flow Model for RELAP5/MOD3 Code, *Annals of Nuclear Energy*, Vol.32, (2005), pp.913–924.
(2) Kuroda, T., Watanabe, T., and Kukita, Y., Break Flow Modeling for a Steam Generator Tube Rupture (SGTR) Incident in a Pressurized Water Reactor (PWR) (in Japanese), *JAERI-M*, Vol.93-236, (1993).
(3) Ransom, V.H., and Trapp, J.A., The RELAP5 Choked Flow Model and Application to a Large Scale Flow Test, *Proceedings of the ANS/ASME/NRC International Topical Meeting on Nuclear Reactor Thermal-Hydraulics*, (1980), pp.799–819.
(4) Städtke, H., Franchello,G., and Worth, B., Numerical Simulation of Multi-Dimensional Two-Phase Flow Based on Flux Vector Splitting, *Nuclear Engineering and Design*, Vol.177, (1997), pp.199–213.
(5) Tiselj, I., Horvat, A., Cerne, G., Gale, J., Parzer, I., Mavko, B., Giot, M., Seynhaeve, J.M., Kucienska, B., and Lemonnier., H., WAHA3 Code Manual, *JSI Report*, Vol.IJS-DP-8841, (2004).
(6) U.S. NRC, TRACE V5.0 Theory Manual Field Equations, Solution Methods, and Physical Models, (2008).
(7) ANSYS, Ansys Fluent 12.0 Theory Guide, (2009).
(8) Schmidt, S.J., Sezal, I., and Schnerr, G.H., Compressible Simulation of High-Speed Hydrodynamics with Phase Change, *Proceedings ECCOMAS CFD 2006*, (2006), pp.451, (in CD-ROM).
(9) ANSYS, Tutorial: Heat and Mass Transfer with the Mixture Model, (2006).
(10) ANSYS, Tutorial 19. Using the Mixture and Eulerian Multiphase Models, (2006).